GUST LOAD PASSIVE ALLEVIATION BY MEANS OF NONLINEAR, BUCKLING DRIVEN, STRUCTURAL RESPONSE

Francesco Toffol[1], Chiara Bisagni[1]

[1]Politecnico di Milano, Department of Aerospace Science and Technology, via la Masa 34, 20156, Milano, Italy

Abstract

This paper presents recent activities conducted in the framework of the ERC-NABUCCO project aimed at increasing the structural efficiency of future aircraft through innovative concepts based on a smart adoption of buckling-driven solutions. While structural buckling has traditionally been viewed as a potentially dangerous phenomenon to be avoided due to its association with catastrophic failure, the nonlinear behavior associated with this phenomenon could actually be beneficial in the current push for more efficient structures. The paper describes how allowing a certain level of buckling in specific locations of a typical wingbox could result in a reduction of peak loads caused by gust response, which typically dictate the structural sizing process, ultimately leading to weight savings.

Keywords: Passive load control, gust loads alleviation, buckling and post-buckling

1. Introduction

The need to explore the benefits of novel aircraft architectures to provide a significant increase in fuel efficiency is evident. This need has been identified by ICAO, FLIGHTPATH2050, Clean Sky 2 and more recently Clean Aviation initiatives in Europe as well as by NASA, with challenging goals set for reductions in CO_2, NO_X and noise by the year 2050 [1-2]. However, the path towards a completely carbon neutral air transport will certainly take several years and will require intermediate steps. Historically, the most significant improvements in jet aircraft efficiency have been related to advancements in the propulsive term associated with the development of high-bypass-ratio turbofan engines. Most recently, the increasing use of high-strength composites promises to reduce weight. Additionally, configuration changes such as increased wingspan can improve the lift-to drag ratio. However, it must be noted out that the integrated nature of aircraft design means that few substantive configuration changes can be made without encountering some multidisciplinary trade-offs. This represents the only way to ensure a net improvement in global efficiency by combining and harmonizing conflicting requirements, such as the weight penalty due to increased aspect ratio, or the combination of different objectives resulting from different disciplines, such as blending passive and active control systems.

Different EU projects [3-4] have already demonstrated that a potential reduction in wing structural weight of around 20 percent is achievable through an aggressive combination of maneuver and gust load alleviation technologies. This reduction in wing structural weight ultimately leads to an overall weight reduction of 4-5% for the entire aircraft, considering the snowball effects. This structural weight reduction could potentially result in produce a fuel burn reduction of the around of 6-8% on a typical short and medium range flight mission.

The ERC Advanced Grant Project NABUCCO (New Adaptive BUCkling-driven COmposite aerospace structures), which began in May 2023, aims to design adaptive buckling-driven structural concepts for the next generation of aircraft. The project aims to achieve this goal by utilizing buckling

phenomena, particularly their nonlinear response and related stiffness redistribution [5], to control responses and induce shape variation.
While it is understood that structural nonlinear responses can reduce the peak loads as in the case of gust responses [6], the potential benefits of introducing these capabilities in the commonly used numerical framework for dynamic aeroelastic response calculation, have not been fully explored. Current numerical approaches used to meet the CS25 certification rules are primarily based on linear aeroelastic analysis tools, which are not immediately applicable in the case of nonlinear responses caused by buckling induced changes in stiffness.
This paper introduces a new methodology to account for the localized nonlinearity introduced by buckling, without compromising the efficiency of commonly used approaches for dynamic loads computation. An example is provided to illustrate the application of this approach in evaluating the impact of buckling on the gust load envelope.

2. Gust Loads Computation Framework

In aircraft design, gust related dynamic load conditions can easily reach 10 millions (e.g. 50 flight points, 100 mass cases, 10 control surface configurations, 50 manoeuvres and gust gradients, 4 control laws), which can be reduced to some thousands thanks to practical engineering judgement, such as using load envelopes to identify more sever conditions. This large number of load cases cannot be analysed with detailed non-linear solutions on high fidelity models, for this reason the typical approach adopted by aerospace industries to determine the complete set of dynamic loads, including those related to continuous and discrete gust conditions, is mainly based on linear methods applied to simplified models.
Usually, a stick model with properties derived from a detailed finite element (FE) model of the aircraft, is coupled with an unsteady aerodynamic solver, typically a Doublet Lattice Method (DLM). Due to the need to analyse thousands of conditions, resulting from different aircraft configurations and flight conditions, the computation scheme is based on the use of a reduced model, which is based on a limited set of vibration modes, and the problem is solved in the frequency domain since the DLM is a frequency-based method [7].
Structural buckling, on the other hand, needs to be treated as a nonlinear problem, especially if the redistribution of stiffness and the associated stresses during the post-buckling regime must be fully understood. In this scenario, a time marching solution seems more appropriate. However, this approach is not ideal for analyzing numerous cases due to its computational expense and time-consuming case set-up. The novelty of this work lies in utilizing conventional preliminary design tools, as described in the next paragraph, but modified to account for the nonlinearity caused by buckling, as outlined in section 3.
The gust analyses are performed using NeoCASS, an aero-servo-elastic simulation tool developed by the Politecnico of Milano [8]. It is based on the stick representation for the structural part (beam elements for structural components and concentrated masses for non-structural items) coupled with a DLM solver for the aerodynamics through a set of splines based on the Radial Basis Functions (RBF) [9].
In the industry, this kind of model is used to compute the static (trim) and dynamic (gust, control surface response, etc.) loads envelope that is used to size the aircraft. Focusing on the gust loads, the stick model is the compromise between accuracy and analysis cost that allows to identify the sizing load set performing a high number of analyses. The overall load set must encompass different flight points (altitude and airspeed) and mass configurations to cover all the aircraft flight conditions.
Dynamic problems are usually solved on a Reduced Order Model (ROM), that is computationally cheaper than solving the problem on the full Degrees of Freedom (DOFs) set. It is common practice for such applications to project the aeroelastic problem on the modal base, that contains the most relevant structural modes. For this reason, in the following the problem is written in modal base where $\boldsymbol{u} = \boldsymbol{U}\boldsymbol{q}$, being **u** the DOFs physical displacement, **U** the eigenvectors matrix and **q** the modal coordinates.
The aerodynamic force computation performed by the DLM is based on the (reduced) frequency domain, and usually the problem is solved in frequency and then translated in time through an inverse Fourier's transformation. The Generalized Aerodynamic Forces (GAFs) due to the structural motion

and gust excitation, obtained as function of reduced frequency (k) and Mach number (Ma) are in the form of Eq.(1), where q_∞ is the dynamic pressure, **q** is the modal displacement, v_g is the gust velocity and $\mathbf{H_{am}}$, $\mathbf{H_{ag}}$ are the aerodynamic matrices related to the structural motion and gust respectively.

$$\boldsymbol{GAFs} = q_\infty(\boldsymbol{H_{am}}(k,Ma)\boldsymbol{q} + \boldsymbol{H_{ag}}(k,Ma)v_g \tag{1}$$

Despite describing functions [10] can be used for the introduction of non-linearities, it is easier, and more general, to introduce them into a state-space (SS) model as described in section 3, but before the frequency dependent GAFs need to be translate in time domain. NeoCASS implements a feature for the identification of the aerodynamic forces transfer function based on the Matrix-Fraction Approximation (MFA) method [11], that approximates the transfer function $\mathbf{H_{am}}$ as function of the non-dimensional Laplace's variable p, as in Eq.(2), where **A**, **B**, **C**, **D** are the aerodynamic system matrices to be identified.

$$\mathbf{H}_{am}(p) \approx \mathbf{D^0}_a + p\mathbf{D^1}_a + p^2\mathbf{D^2}_a + \mathbf{C}_a(p\mathbf{I} - \mathbf{A}_a)^{-1}\left(\mathbf{B^0}_a + p\mathbf{B^1}_a + p^2\mathbf{B^2}_a\right) \tag{2}$$

Once identified the **A**, **B**, **C**, **D** matrices, it is possible to reformulate Eq.(2) into Eq.(3), substituting the Laplace variable *p* with the time derivatives$\left(\frac{dz}{dt} = \dot{z}\right)$. The result is a state-space system where $\mathbf{x_a}$ is the aerodynamic state, **q** are the modal displacements and $\mathbf{Q_a}$ are the aerodynamic forces due to the structural motion.

$$\begin{cases} \dfrac{d\mathbf{x}_a}{dt} & = \dfrac{1}{t_a}\mathbf{A}_a\mathbf{x}_a + \dfrac{1}{t_a}\mathbf{B^0}_a\mathbf{q} + \mathbf{B^1}_a\dot{\mathbf{q}} + t_a\mathbf{B^2}_a\ddot{\mathbf{q}} \\ \mathbf{Q_a} & = \mathbf{C}_a\mathbf{x}_a + \mathbf{D^0}_a\mathbf{q} + t_a\mathbf{D^1}_a\dot{\mathbf{q}} + t_a^2\mathbf{D^2}_a\ddot{\mathbf{q}} \end{cases} \rightarrow \begin{cases} \dot{\mathbf{x}}_a & = \mathbf{A}\mathbf{x_a} + \mathbf{B}\mathbf{q} \\ \boldsymbol{Q_a} & = \mathbf{C}\mathbf{x_a} + \mathbf{D}\mathbf{q} \end{cases} \tag{3}$$

A similar approach is used for the definition of the gust related term of the GAFs, $\mathbf{H_{ag}}$.
The resulting aerodynamic system is coupled with the structural SS model derived from the classical mechanical equations of an elastic system projected on a modal base, characterized by modal mass ($\mathbf{M_{hh}}$), damping ($\mathbf{C_{hh}}$), and stiffness ($\mathbf{K_{hh}}$) matrices.
The state of the mechanical system (modal motion **q**) is the input for the aerodynamic SS system, and the modal aerodynamic forces ($\mathbf{Q_a}$) are the forcing term of the mechanical system. The two SS model can be assembled into a single SS model, generating an aero-elastic SS model, completely defined in the time domain, as in Eq.(4), where the external forcing term $\mathbf{F_c}$ is added.

$$\begin{bmatrix} \mathbf{I} & \mathbf{0} & \mathbf{0} \\ \mathbf{0} & \mathbf{M_{hh}} - q_\infty t_a^2\mathbf{D^2}_a & \mathbf{0} \\ \mathbf{0} & -t_a^2\mathbf{B^2}_a & t_a\mathbf{I} \end{bmatrix} \frac{d}{dt}\begin{bmatrix} \mathbf{q} \\ \dot{\mathbf{q}} \\ \mathbf{x}_a \end{bmatrix} =$$
$$+ \begin{bmatrix} \mathbf{0} & \mathbf{I} & \mathbf{0} \\ -\left(\mathbf{K_{hh}} - q_\infty\mathbf{D^0}_a\right) & -\left(\mathbf{C_{hh}} - q_\infty t_a\mathbf{D^1}_a\right) & q_\infty\mathbf{C}_{a+g} \\ \mathbf{B^0}_a & t_a\mathbf{B^1}_a & \mathbf{A}_{a+g} \end{bmatrix} \begin{bmatrix} \mathbf{q} \\ \dot{\mathbf{q}} \\ \mathbf{x}_{a+g} \end{bmatrix} \tag{4}$$
$$+ \frac{1}{V_\infty}\begin{bmatrix} \mathbf{0} & \mathbf{0} & \mathbf{0} \\ q_\infty\mathbf{D^0}_{ag} & q_\infty t_a\mathbf{D^1}_{ag} & q_\infty t_a^2\mathbf{D^2}_{ag} \\ \mathbf{B^0}_{ag} & t_a\mathbf{B^1}_{ag} & t_a^2\mathbf{B^2}_{ag} \end{bmatrix} \begin{bmatrix} v_g \\ \dot{v}_g \\ \ddot{v}_g \end{bmatrix} + \begin{bmatrix} \boldsymbol{B_c} \\ 0 \\ 0 \end{bmatrix} [\mathbf{F_c}]$$

Finally, the SS model can be converted into the canonical form of Eq.(5), where the aeroelastic state $\mathbf{x_{ae}}$ contains both mechanical and aerodynamic states, the inputs are the gust profile alongside its time derivatives $\mathbf{u_g}$, and the control force $\mathbf{u_c}$. The output **y** is whichever required structural response.

$$\begin{cases} \dot{\boldsymbol{x}}_{ae} = \boldsymbol{A}\boldsymbol{x}_{ae} + \boldsymbol{B}_g\boldsymbol{u}_g + \boldsymbol{B}_c\boldsymbol{u}_c \\ \boldsymbol{y} = \boldsymbol{C}\boldsymbol{x}_{ae} + \boldsymbol{D}_g\boldsymbol{u}_g + \boldsymbol{D}_c\boldsymbol{u}_c \end{cases} \tag{5}$$

The obtained SS model can be used to perform aeroelastic gust responses directly in time domain, and since the native environment of NeoCASS is Matlab, the implementation of a Simulink model is straightforward. The model is Linear Time Invariant (LTI), but it can be modified to introduce concentrated nonlinearities as described in the next section.

3. Buckling-Driven Nonlinear Aeroelastic Response

This section describes how the nonlinearity generated by the buckling is accounted into an aeroelastic simulation based on a LTI SS model. The typical behaviour of a stiffened panel in pre and post buckling conditions is reported in Figure 1: the non-linear relationship between the force and the displacement has a bi-linear behaviour [12-13], characterized by the two linear stiffness values and the point at which buckling occurs. For a stick model, which reduces the 3D model of the wingbox into a 1D beam element, this is equivalent to a localized stiffness modification in correspondence of the area where buckling occours.

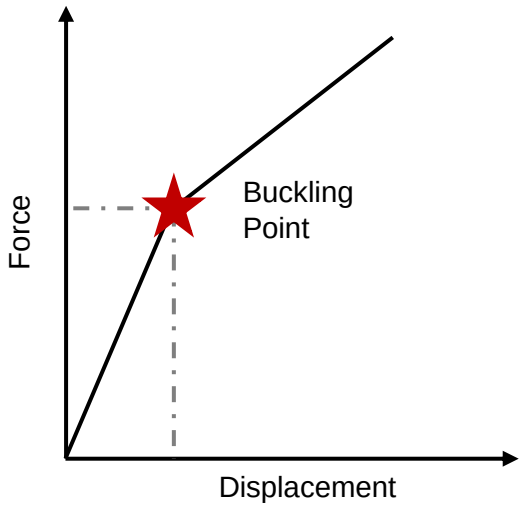

Figure 1: Typical non-linear behaviour of pre- and post-buckling force-displacement relation

The implementation of such stiffness behaviour into the structural model is not straightforward, for this reason a time-marching approach derived to the one used in [14-16] is used. The basic idea is represented in Figure 2, and consists in replacing the stiffness between two elements with a control force that is function of the relative displacement itself. This feedback force acts as a "numerical" spring that connects the DOFs involved by the buckling, that feeds back a force or moment. Figure 2 sketches the approach for a simple 1DOFs mass-spring system, where the linear spring is removed from the system and it is replaced by a force F, proportional to the displacement x through the stiffness value k itself, but the concept can be easily extended to a FE model.

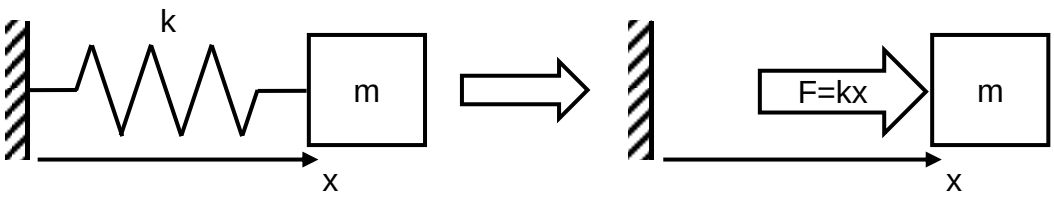

Figure 2: Schematic representation of the proposed approach

This control-like approach allows to use a feedback force that is no more linearly dependent on the displacement, but it can be an arbitrary function of the structural response, transforming the classical Hooke's law $F = kx$ into a more general $F = f(x)$.

The feedback branch is added to the SS model realized following the approach described in Section 2, resulting in the Simulink block scheme of Figure 3.

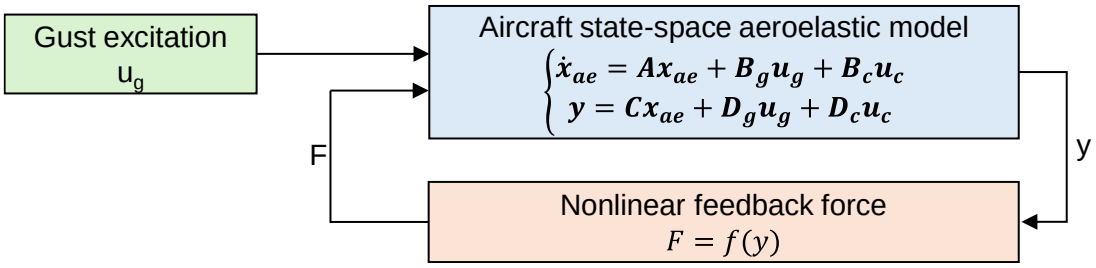

Figure 3: Simulink model for the force feedback

The displacement-force relation of Figure 1 is implemented as in Eq.(6), where F is either a force or a moment, k is the stiffness in pre and post buckling (b) conditions, x is the relative motion between two DOFs (either a translation or a rotation), P_b and x_b are respectively the buckling load and the related displacement.

$$\begin{cases} F = k_{pre\ b} x \ for\ x < x_b \\ F = k_{post\ b} x + P_b - k_{post\ b} x_b \ for\ x > x_b \end{cases} \quad (6)$$

The bilinear stiffness behaviour assumed for this work can be easily replaced with an arbitrary stiffness distribution. With a more general perspective, the feedback can be an arbitrary function of whicheverer structural response, for example in the case of a nonlinear damping that is function of the velocity.

To implement such feedback, the kinematic of the stick structure has to be modified. In the area where the buckling is supposed to appear, two coincident nodes are placed. The kinematic is modelled with an algebraic constraint (MPC) for the degrees of freedom (DOFs) that are not affected by the buckling, while the remaining DOFs remain unconstrained, and a scalar point (SPOINT) is added to the equation. A scheme of the kinematic is presented in Figure 4, while the MPC relation is expressed as in Eq.(7), where x_i is the displacement of the i-th DOF for the nodes A and B.

$$\begin{cases} x_{A,i} = -x_{B,i} \rightarrow for\ non-buckled\ DOFs \\ x_{A,i} = -x_{B,i} - x_{SPOINT} \rightarrow for\ buckled\ DOF \end{cases} \quad (7)$$

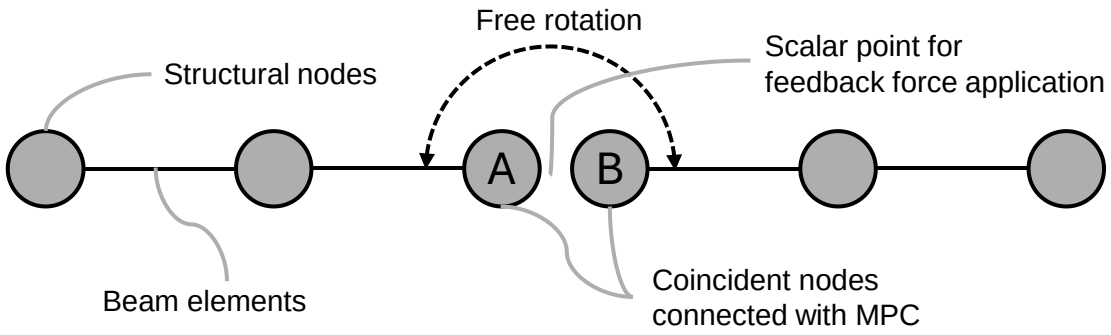

Figure 4: Kinematics used for the introduction of the nonlinear force

The kinematic is restored by forcing the scalar point through the value obtained with Eq.(6). In this case the relative displacement between A and B is the displacement of the scalar point. For the linear case, the force is proportional to the displacement or rotation through the stiffness: $F = -Kx$. In the case a non-linear phenomenon, like when buckling occurs, the stiffness may be an arbitrary function of the scalar point displacement: $F = f(x)$. Figure 3 shows the Simulink's block diagram of the proposed simulation framework, where x is the scalar point displacement used as feedback measure

and the computed nonlinear force F restores the kinematics.
The framework, developed for simple stick structures, helps to understand the impact of the buckling on the aeroelastic response. A non-linear time marching simulation of a full wing is a computationally expensive simulation that cannot be used for trade-off and sensitivity studies. Instead of evaluating the force vs. displacement function as a result of a detailed analysis, the proposed framework helps the designer to evaluate how the response is affected by the buckling load and by the stiffness reduction in post-buckling conditions. It must be considered as part of a wider design loop, represented in Figure 5: the aeroelastic simulation on a simplified model provides indications about the desired buckling behaviour, while the next design steps, performed on higher fidelity models, must design a structure that buckle as prescribed. It is a buckling-driven design because the objective of the high-fidelity optimisation is the buckling behaviour that is identified on a lower fidelity model and computationally cheap aeroelastic framework. After the first set of high-fidelity analyses, the stick model is updated with the buckling behaviour identified, iterating the loop until the convergency is reached.

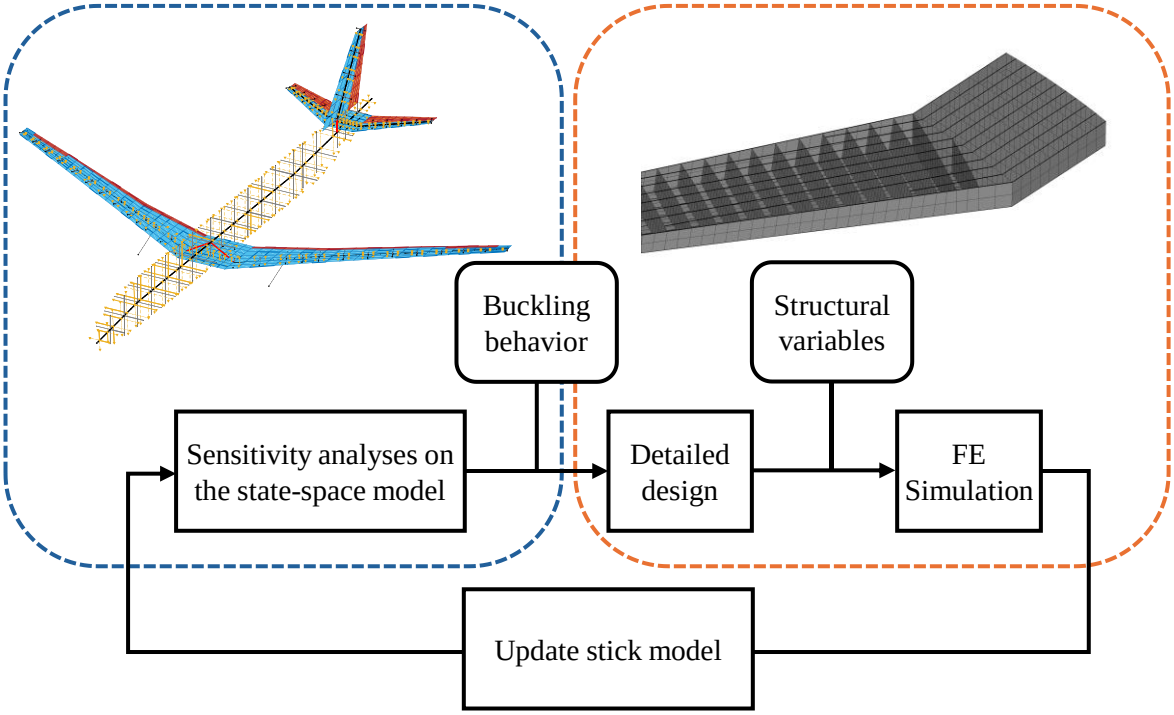

Figure 5: Buckling Driven Design Approach and the models used in each phase.

The description of the detailed design performed on the higher fidelity FE model is not presented in this work, that is mainly focused on the development of the non-linear aeroelastic simulation framework.

4. Application

The framework described in Section 3 is here exploited to investigate the gust response of a clamped wing. This boundary condition addresses the focus on the aeroelastic response without considering eventual contribution coming from rigid body modes. However, the wing is fully representative of a medium range aircraft, and it was extracted from a model studied within the U-HARWARD [4], where an aircraft like the Airbus A321 with an aspect ratio extended to AR=15 was considered.
Figure 6(a) shows the CAD model of the full aircraft, while Figure 6(b) represents the aeroelastic model of the clamped wing, with indicated the area where the buckling is considered. It is the wing root and in this region the model is modified to introduce the coincident nodes to modify the kinematics.

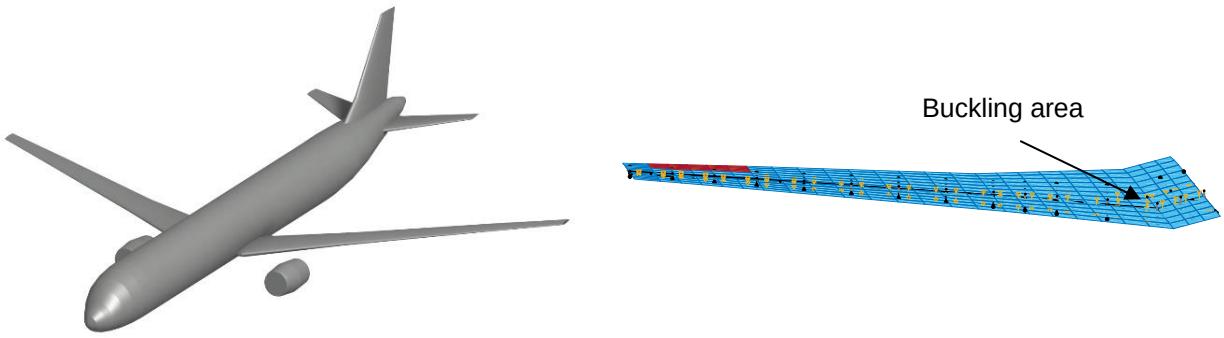

(a) CAD model of the A321 AR15 aircraft

(b) Aeroelastic Stick model with DLM mesh of the A321 AR15 wing

Figure 6: Reference models.

A parametric study was performed using as mean of comparison the Wing Root Bending Moment (WRBM): its sensitivity w.r.t. the buckling load (parameter 1, P1) and the post buckling stiffness (parameter 2, P2) for several gusts was mapped. The impact of P1 and P2 on the stiffness is reported in Figure 7(a). The buckling load, or P1, ranged between the maximum feedback force for the linear case and 50% of this value. At the same time, the post-buckling stiffness, or P2, was reduced from 0% to 50% w.r.t. the nominal case. For both cases, a discretization of 10% was used, creating a total of 5 P1 x 5 P2 = 25 nonlinear stiffness curves. This led to investigate force-displacement functions that cover the grey-filled area of Figure 7(b), where the starred marker indicates the maximum load acting on the scalar point for the linear case and the related displacement, value adopted to non-dimensionalize the plot.

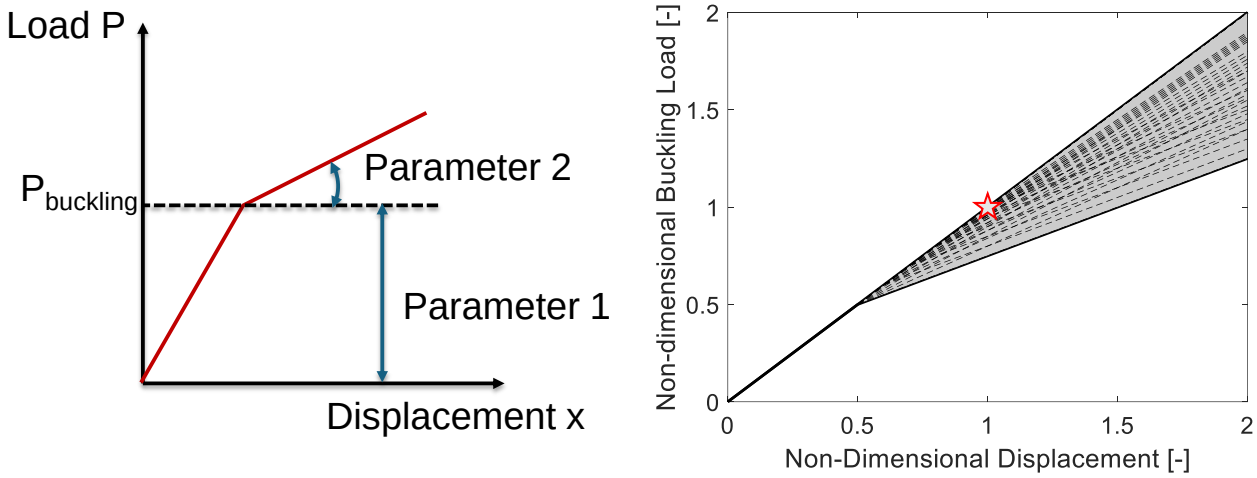

(a) Parameters used in the sensitivity analysis

(b) Maps of the nonlinear stiffnesses considered

Figure 7: Maps of the force-displacement considered during the sensitivity study.

All the 25 models were excited using 10 different gust lengths with positive and negative amplitudes following CS/EASA 25 regulation for large transportation aircraft. It resulted in the gust profile represented in Figure 8 (only positive gust plotted). It was selected a single flight point, equivalent to the cruise condition with a true air speed (TAS) of 229m/s at an altitude of 8000m.

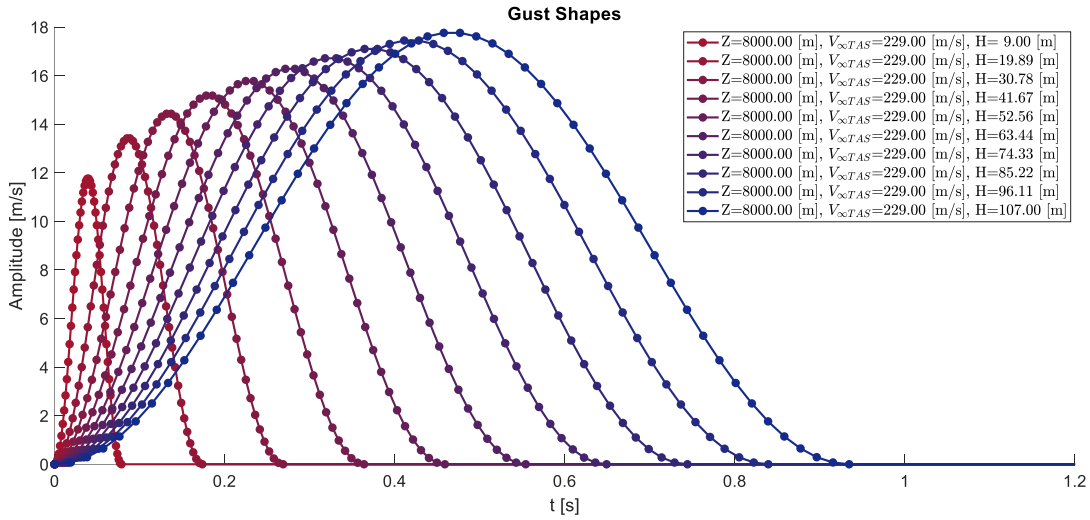

Figure 8: 1-cosine gust shape considered for the analyses.

For each gust and P1/P2 combination, it is possible to recover the time history of the quantity of interest, in this case of the WRBM. As an example, the time response of the feedback force for different buckling cases (grey lines) are compared with the linear case (red line) in Figure 9.

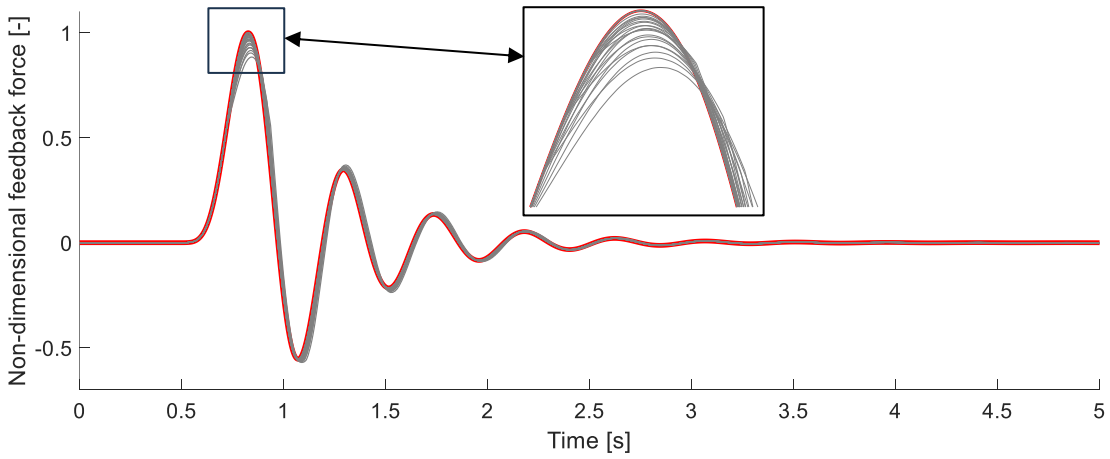

Figure 9: Feedback force for different buckling cases

The simulations show a reduction of the feedback force, that directly impact on the WRBM, but the interpretation of the results from the time histories is hard to read. For this reason, for each model analyzed, the maximum WRBM is compared with the one obtained in the linear case, resulting into the sensitivity map of

Figure 10, that shows how the WRBM peak is affected by P1 (buckling load) and P2 (stiffness reduction). Both the parameters concur to alleviate the WRBM peak, obtaining a passive alleviation up to 10%. It is possible to notice how the same WRBM alleviation can be obtained considering different P1&P2 combinations (isolines in

Figure 10), this set of information is then provided to the next design phases to investigate which is the best structural solution to achieve the desired alleviation.

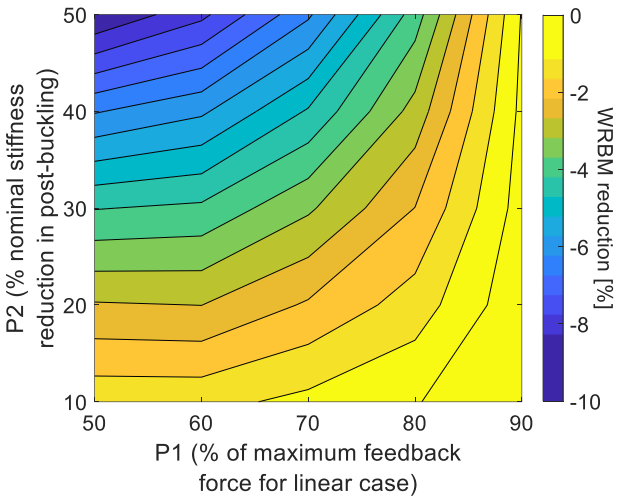

Figure 10: Sensitivity of the WRBM peak w.r.t. P1 and P2

5. Conclusions

This work proposes a simple but effective approach to consider local nonlinearities, such as stiffness reduction in the post-buckling regime, for gust load alleviation. The approach works with the model conventionally adopted in conceptual-preliminary design phases for dynamic load computation (stick + DLM). It increases the analysis capability by considering a phenomenon, buckling, that is typically investigated with more computationally expensive analysis and more complex models. This allows for the analyse of many configurations, in the order of thousands, in a reasonable time and with limited computational resources, like a notebook. The approach can be used to a) establish the desired buckling performances to be achieved with a detailed optimization, and to b) evaluate the dynamic response of a structure with provided buckling behaviour. It is easy to establish a design loop between the two design steps.

The application of the proposed approach to a conventional wing shows how remarkable (10%) WRBM reductions can be achieved by exploiting buckling, rather than treating it as a phenomenon to be avoided. Different combination of buckling load and stiffness reduction provide the same alleviation capability, opening a design space to find the optimal compromise between the structural solution and buckling performance.

The results presented are the first step of the NABUCCO's project, which will promote the buckling-driven design to realize more efficient structural solutions.

6. Acknowledgements

Funded by the European Union (ERC Advanced Grant, NABUCCO, project number 101053309). Views and opinions expressed are however those of the authors only and do not necessarily reflect those of the European Union or the European Research Council Executive Agency. Neither the European Union nor the granting authority can be held responsible for them.

7. Contact Authors Email Address

Francesco Toffol, PhD: francesco.toffol@polimi.it

Prof. Chiara Bisagni: chiara.bisagni@polimi.it

8. Copyright Statement

References

[1] *European Commission, Directorate-General for Mobility and Transport, Directorate-General for Research and Innovation, Flightpath 2050: Europe's Vision for Aviation: Maintaining Global Leadership and Serving Society's Needs, Publications Office, 2011.*

[2] *European Commission, Directorate-General for Research and Innovation, Strategic Research and Innovation Agenda (SRIA) of the European Open Science Cloud (EOSC), Publications Office of the European Union, 2022.*

[3] *Toffol F. and Ricci, S. Development of an active wingtip for aeroelastic control. Aerospace, Vol. 10, No. 8, pp. 693 (24 pages), 2023.*

[4] *Marchetti L., Toffol F., Ricci S., Beretta J. and Paletta N. Aeroelastic optimization of high aspect ratio wings for environmentally friendly aircraft. Proc. AIAA Scitech 2022, San Diego, January 3-7, 2022.*

[5] *Zhang J. and Bisagni C. Buckling-driven mechanisms for twisting control in adaptive composite wings, Aerospace Science and Technology, Vol. 118, 107006, 2021.*

[6] *Hahn D. and Haupt M. Exploration of the effect of wing component post-buckling on bending-twist coupling for nonlinear wing twist. CEAS Aeronautical Journal, Vol. 13, pp. 663-676, 2022.*

[7] *Albano E. and Rodden W. P. A doublet-lattice method for calculating lift distributions on oscillating surfaces in subsonic flows. AIAA Journal, vol. 7, no. 2, pp. 279–285, 1969.*

[8] *Cavagna L., Ricci S. and Travaglini L. NeoCASS: An integrated tool for structural sizing, aeroelastic analysis and MDO at conceptual design level. Progress in Aerospace Sciences, Vol. 47, No. 8, 2011, pp. 621-635, 2011.*

[9] *Beckert A. and Wendland, H. (2001). Multivariate interpolation for fluid-structure-interaction problems using radial basis functions. Aerospace Science and Technology, 5(2), 125-134.*

[10] *Gelb A. Multiple-Input Describing Functions and Nonlinear System Design. p. 661, 1968.*

[11] *Ripepi M. and Mantegazza P. Improved matrix fraction approximation of aerodynamic transfer matrices. AIAA Journal, Vol. 51, No. 5, pp 1156-1173, 2013.*

[12] *van Dooren K. S., Bas T., Waleson J.E.A. and Bisagni C. Skin-stringer separation in post-buckling of butt-joint stiffened thermoplastic composite panels. Composite Structures, Vol. 304, 116294304, 2023.*

[13] *van Dooren K.S. and Bisagni C. Design, analysis and testing of thermoplastic welded stiffened panels to investigate skin-stringer separation in post-buckling. Composites Part B, Vol. 267, 111033, 2023.*

[14] *Fonzi N. Limit Cycle Oscillations due to Control Surface Freeplay: Analysis Methods and Physical Insight, PhD Thesis, Politecnico di Milano, 2023*

[15] *Conner M. D., Tang D. M., Dowell E. H. and Virgin L. N. Nonlinear behavior of a typical airfoil section with control surface freeplay: a numerical and experimental study. Journal of Fluids and Structures, vol. 11, no. 1, pp. 89–109, 1997. Number: 1 Publisher: Elsevier.*

[16] *Silva G. H. C., Rossetto G. D. B. Dimitriadis G. Reduced-Order Analysis of Aeroelastic Systems with Freeplay Using an Augmented Modal Basis. Journal of Aircraft, vol. 52, pp. 1312–1325, Dec. 2014. Number: 4 Publisher: American Institute of Aeronautics and Astronautics.*